THE JOURNAL OF PHYSICAL CHEMISTRY LETTERS
A JOURNAL OF THE AMERICAN CHEMICAL SOCIETY

pubs.acs.org/JPCL Letter

Allegro-FM: Toward an Equivariant Foundation Model for Exascale Molecular Dynamics Simulations

Ken-ichi Nomura,* Shinnosuke Hattori,* Satoshi Ohmura, Ikumi Kanemasu, Kohei Shimamura, Nabankur Dasgupta, Aiichiro Nakano, Rajiv K. Kalia, and Priya Vashishta

Cite This: J. Phys. Chem. Lett. 2025, 16, 6637−6644 Read Online

ACCESS | Metrics & More | Article Recommendations | Supporting Information

ABSTRACT: We present a foundation model for exascale molecular dynamics simulations by leveraging an E(3) equivariant network architecture (Allegro) and a set of large-scale organic and inorganic materials data sets merged by the Total Energy Alignment framework. The obtained model (Allegro-FM) is versatile for various material simulations for diverse downstream tasks covering 89 elements in the training sets. Allegro-FM exhibits excellent agreement with high-level quantum chemistry theories in describing structural, mechanical, and thermodynamic properties, while exhibiting emergent capabilities for structural correlations, reaction kinetics, mechanical strengths, fracture, and solid/liquid dissolution, for which the model has not been trained. Furthermore, we demonstrate the robust predictability and generalizability of Allegro-FM for chemical reactions using Transition1x, which consists of tens of thousands of organic reactions and 9.6 million configurations including transition state data, in addition to reactive simulations using calcium silicate hydrates as a test bed. With its computationally efficient, strictly local network architecture, Allegro-FM scales up to multibillion-atom systems with a parallel efficiency of 0.975 on the exaflop/s Aurora supercomputer at Argonne Leadership Computing Facility. The approach presented in this work demonstrates the potential of the foundation model for novel materials design and discovery based on large-scale atomistic simulations.

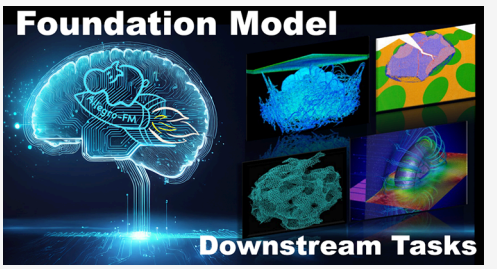

The foundation model (FM) is a paradigm shift in artificial intelligence (AI)[1] and has transformed our way of model training. Unlike conventional approaches that use domain-specific data sets to perform a well-targeted single task, FMs are trained with massive data sets without a specific target application in mind. A well-trained FM, also called pretrained model, acquires the robustness and generalizability for out-of-distribution tasks, enabling diverse downstream tasks by fine-tuning with relatively small data sets. The concept of the FM originates from large language models (LLMs), such as OpenAI ChatGPT,[2,3] Google Gemini,[4] and Meta LLaMA.[5] With the unprecedented success of LLMs, FM that is capable of performing versatile tasks with multimodal input data has gained traction in many research fields including materials and chemical sciences.[6,7]

There are two key components for a successful FM development, i.e., advanced model architecture and large-scale data sets. Transformer network equipped with the attention mechanism[8] has been widely used in LLMs with hundreds of billions of learnable parameters trained on millions of tokens. Self-supervised learning is one of the enabling technologies for such LLMs by eliminating the laborious and expensive data labeling. Fine-tuning is a form of transfer learning, in which a part of the network weights in the pretrained model are adjusted by a separately prepared smaller data set for specialized tasks.

FM has several significant advantages over conventional models developed for a narrowly defined task. Although generating an FM is extremely resource-intensive, a well-trained FM may be fine-tuned with much fewer resources, enabling even a user with a very modest computing resource to incorporate the model in their workflow. Also, FMs are used as a base model for versatile downstream tasks.[1] As such, it is not necessary to develop a new model from scratch for a different downstream application, thereby reducing the total cost and time investment.

Recently, great strides have been made in terms of both model architecture and training data sets for materials modeling and simulations. Many large-scale data sets such as Materials Project,[9,10] SPICE,[11] ANI, Alexandria,[12] OQMD,[13] and AFLOW[14] are publicly available. Modern architectures take advantage of Graph Neural Network (GNN), multibody expansion strategy, and the equivariant features from molecular geometry (ACE,[15] MACE,[16] Nequip,[17] Equiformer,[18,19] Orb,[20] and MatterGen[21]). The model expressibility has increased

Received: February 26, 2025
Revised: May 19, 2025
Accepted: May 20, 2025
Published: June 20, 2025

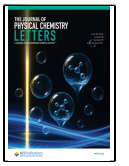

https://doi.org/10.1021/acs.jpclett.5c00605
J. Phys. Chem. Lett. 2025, 16, 6637−6644

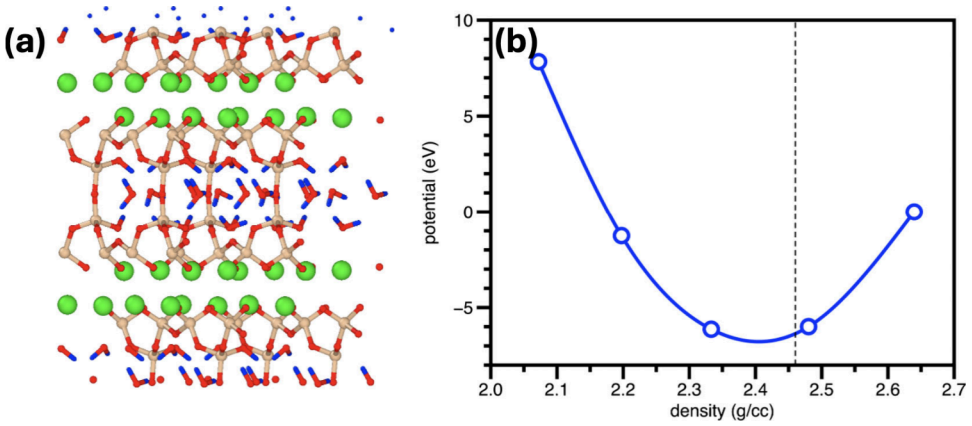

Figure 1. (a) Snapshot of the tobermorite 11 Å (T11) structure. Green, khaki, red, and blue spheres represent Ca, Si, O, and H atoms, respectively. (b) Equation of state of T11 using Allegro-FM. The dotted-line shows an experimental density of T11 at 2.46 g/cm^3.[48]

substantially along with the number of learnable parameters. Current state-of-the-art (SOTA) models are based on multimillion training parameters.[22] While the emerging trend of FMs for atomistic simulation is evident, this novel approach poses scientific questions as well as research opportunities, for example, can we develop computationally efficient machine-learning force fields (MLFFs) for a broad set of materials properties and processes?[23] Also lacking to date is a scalable FM that enables molecular dynamics (MD) simulations involving multibillion atoms on exaflop/s parallel supercomputers.

In this study, we present Allegro-FM, a foundation model for exascalable Molecular Dynamics (MD) simulations, employing the linear-scaling and computationally efficient Allegro[24] architecture trained on MPtrj[9] and OFF23 data set[25] aligned with Total Energy Alignment (TEA) framework.[26]

Materials simulations often require a large number of atoms to describe key features, such as dislocation, grain boundaries, distinct phases, and phase boundaries. At the same time, the model should accurately describe the chemical reactions. Allegro achieves SOTA accuracy and speed based on E(3) group-theoretical equivariance and local descriptors, while its excellent stability for large-scale, long-time trajectories (or fidelity scaling) can further be enhanced by sharpness-aware training as in the Allegro-Legato model.[27] Materials data sets are often divided into two categories: organic molecules and inorganic crystals. They are generated with different levels of QM theories and functionals, making them incompatible within single model training.[26] TEA framework smoothly connects the potential energy landscapes between distinct data sets, eliminating the need for expensive data regenerations. TEA achieves consistent data fusion encompassing multiple computational methods through shift-scale (or affine) transformation in a metamodel space,[28] which in turn is rooted in free-energy perturbation[29] and multiscale quantum-mechanics/molecular-mechanics (QM/MM) methods.[30,31]

With the SOTA scalability[32] demonstrated on the Perlmutter supercomputer at the National Energy Research Scientific Computing Center (NERSC), Allegro has a great potential for materials simulations that require million-to-billion atoms.[33−35] As a test bed, we apply Allegro-FM to a tobermorite 11 Å (T11), a representative system of calcium silicate hydrates and its aqueous reactions. Among silicate materials, calcium silicates are important because of their abundance in the Earth's crust as well as being the primary constituent in cement. Since many forms of calcium silicates and their hydrates coexist in cementitious materials, the T11 crystal is often chosen as a representative structure. Aluminum-substituted tobermorites are also found in ancient Roman concrete and thought to be a key ingredient responsible for its robustness and longevity.[36,37]

Recently, cement also attracted attention as a carbon-storage material because of the ability to trap carbon by the mineralization process.[38] CO_2 mineralization naturally occurs as part of the geochemical cycle,[39] and the mechanism has been extensively studied over the years. A mechanistic understanding of CO_2 mineralization is crucial for ensuring safe and long-term carbon storage without gas leakage.[40] Although the carbonation of silicates is detrimental to cement through the loss of mechanical strength and eventual fracture, a recent study presented alternative binder materials to mitigate the issue.[41]

First-principles Quantum MD (QMD)[42,43] simulations provide atomistic-level insights that complement experimental observations. Density Functional Theory (DFT)[44,45] has been routinely used to access a wide range of materials properties although the high computational cost and suboptimal algorithmic scalability prohibits performing simulations spanning a sufficiently long time and large scale to study rich chemistry in cementitious materials. CLAYFF,[46,47] a widely used empirical force field (FF), has been developed for multicomponent minerals and their hydrates. Because of the computational efficiency, CLAYFF allows incorporating complex geometries of minerals and their fluid interfaces. As an empirical FF, however, CLAYFF also suffers from a poor description of chemical reactions and limited transferability. Here, a scalable FM is promising to describe both quantum-mechanically accurate materials properties and chemical reactions for spatially nonhomogeneous systems.

First, we have examined the structural and mechanical properties of the T11 crystal shown in Figure 1a. The T11 structure consists of layers of calcium ions and a covalently bonded Si−O network containing H_2O molecules. Figure 1b presents the equation of state of T11 using Allegro-FM. The obtained mass density at 2.44 g/cm^3 agrees well with an experimental value of 2.46 g/cm^3.[48] Using the Birch−Murnaghan equation of state, the bulk modulus is estimated at 60 GPa by Allegro-FM, which reasonably compares to the bulk modulus of 52.7−60.8 GPa using first-principles and empirical FF calculations.[49−51]

https://doi.org/10.1021/acs.jpclett.5c00605
J. Phys. Chem. Lett. 2025, 16, 6637−6644

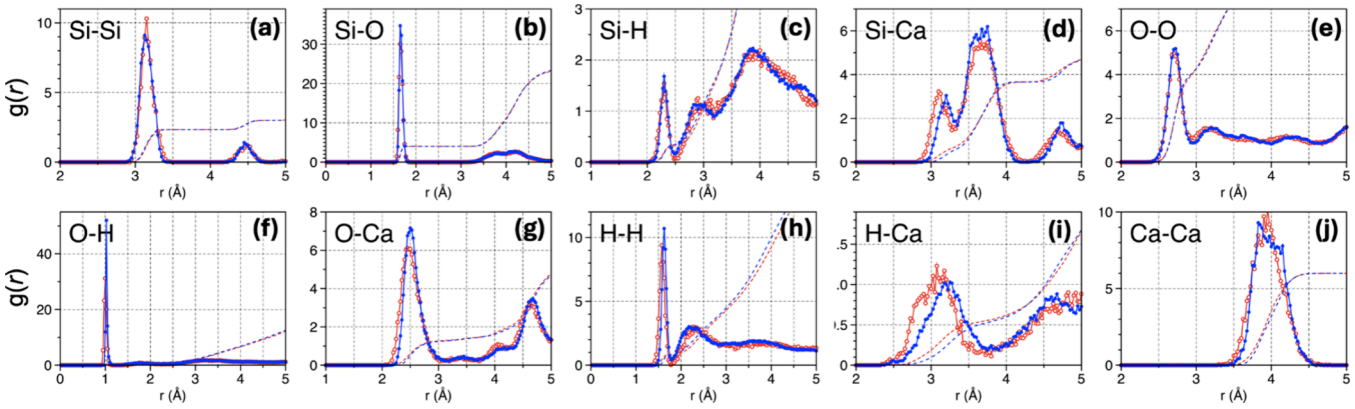

Figure 2. (a–j) Pair distribution function $g(r)$ (solid line) and the coordination numbers $N(r)$ (dotted line) of the T11 crystal using Allegro-FM256 (blue) and QMD (red). $g(r)$ and $N(r)$ are shown with the same vertical scale for atomic pairs indicated in the left top corner of each panel. The system is thermalized at temperature 300 K with the canonical (NVT) ensemble. Beside the peaks in $g(r)$, Allegro-FM accurately reproduces the extent of thermal motion including H_2O molecules. All calculations are performed using Allegro-FM256 (see Table 1).

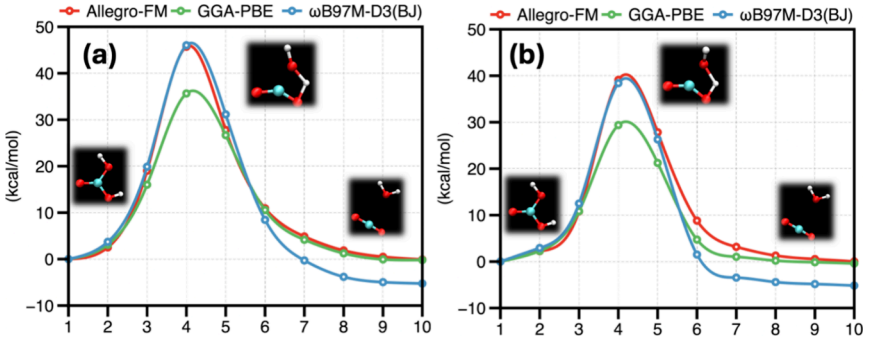

Figure 3. Horizontal and vertical axes show reaction coordinates and activation energies of the decomposition reaction of a carbonic acid into H_2O and CO_2 molecules, respectively. (a and b) Two distinct reaction pathways described in the main text are shown. The inset images show the atomic configurations of initial, transition, and final states obtained by NEB calculation. Red, cyan, and white spheres represent O, C, and H atoms, respectively. All results are aligned by the initial state energy as reference. All calculations are performed using Allegro-FM256 (see Table 1).

Figure 2a–j shows the pair distribution function $g(r)$ and the coordination number $N(r)$ of T11 crystal thermalized at temperature of 300 K using QMD and Allegro-FM. Overall, $g(r)$ and $N(r)$ curves using Allegro-FM and QMD agree well. This result is somewhat expected because the thermal motion of atoms at an ambient condition would not be much different from the distribution in the training data set. Nonetheless, the result also demonstrates the capability of Allegro-FM even without fine-tuning to accurately describe not only the static crystal structure but also the thermal motion of atoms at moderate temperature.

Accurate description of chemical reactions, whether an MLFF can describe bond breaking and formation events, is a great challenge because training data sets are generated near ground states in general. Also, it is not realistic to create a database that contains all necessary information on chemical reactions for a target application, such as the multistep reactions in cement chemistry or geochemical cycles. It is basically a zero-shot learning task that requires out-of-distribution generalizability from the training set. Here, we have examined the predictability of chemical reactions by Allegro-FM using the decomposition of carbonic acid into H_2O and CO_2 molecules as a representative chemical reaction (Figure 3). With reaction coordinates obtained by Nudged Elastic Band (NEB) calculation[52] using the GGA-PBE functional, we have evaluated its energy profile using Allegro-FM, DFT with GGA-PBE, and ωB97M-D3(BJ) that is a hybrid exact-exchange functional with dispersion correlation. We present two distinct reaction pathways: (1) the conventional pathway that is confined within a two-dimensional plane (Figure 3a) and (2) another pathway involving the rotation of the H_2O molecule (Figure 3b).

First, Allegro-FM and ωB97M-D3(BJ) agree well with the transition state (TS) energy. The result may be attributed to the OFF23 data set that is generated with ωB97M-D3(BJ) functional calculations for organic molecules. On the other hand, GGA-PBE and Allegro-FM agree well on the energy of initial and final states, which differs by about 5 kcal/mol using ωB97M-D3(BJ). Overall Allegro-FM generalizes well to TS, providing the activation energy of 45.7 kcal/mol, while 46.0 kcal/mol with ωB97M-D3(BJ), and 35.7 kcal/mol with GGA-PBE for the conventional pathway, respectively. More systematic analysis with the Transition1x[53] data set is also provided in the Supporting Information (see Figure S1 and Table S1).

In order for MLFF to be a viable method for scientific discovery, it must provide a robust MD trajectory well beyond the distribution of training sets. A number of studies have reported that a high prediction accuracy does not warrant the robustness in dynamical simulations;[27,54] for example, MD simulation may fail in an abrupt and unpredictable manner even though an MLFF shows the best benchmark performance.[54] To examine the accuracy and robustness of the MD trajectory with Allegro-FM, we present two simulation results:

https://doi.org/10.1021/acs.jpclett.5c00605
J. Phys. Chem. Lett. 2025, 16, 6637–6644

(1) a tensile test on the T11 crystal and (2) a tobermorite nanoparticle (TNP) immersed in a mixture of H_2O and CO_2 molecules at an elevated temperature of 1200 K.

The fracture mechanics of silicate materials have been extensively studied due to the technological importance as well as its fundamental scientific questions.[55−58] To examine the fracture behavior of T11 crystal, we have performed tensile loading simulation along the *c*-axis that involves the lowest-energy surface[59] and validated by QMD simulation with GGA-PBE functional. Figure 4a shows the stress−strain curve

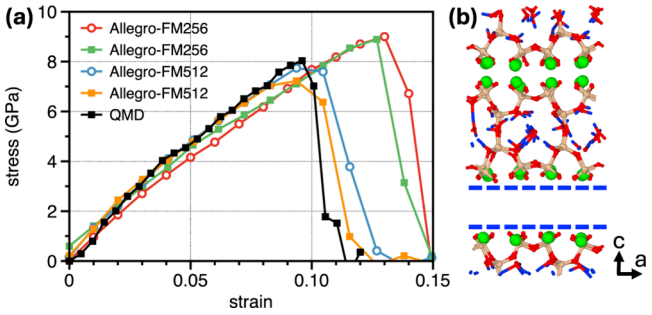

Figure 4. Tensile test on the T11 system thermalized at 300 K. (a) Stress−strain curves with QMD, Allegro-FM with two different model sizes (256 and 512). We have examined two strain rates, 10^{10} s^{-1} (open circles) and 5×10^9 s^{-1} (solid squares), that do not exhibit noticeable difference in the stress−strain curve. The abrupt drop in stress value indicates a brittle fracture. (b) Screenshot of a fractured T11 crystal. Blue-dotted lines indicate its cleavage plane at the Ca double layer.

obtained by QMD and Allegro-FM. The system is thermalized at 300 K and subjected to a tensile strain along the *c*-axis. We have tested two model sizes (Allegro-FM256 and Allegro-FM512) and two strain rates, 10^{10} s^{-1} and 5×10^9 s^{-1}. Overall, all systems show a clean cleavage plane between the calcium double layer. Allegro-FM and QMD show virtually identical results in the elastic regime with a small strain. While the effect of strain rate using Allegro-FM256 is almost negligible, the T11 system fractured at a strain of 0.13, which is 30% larger than the QMD result. Allegro-FM512 in turn shows a nearly identical result with QMD: a brittle fracture at 11% strain (see Figure 4b).

Carbonation of silicates at the solid−liquid interface involves multistep chemical reactions and is affected by many factors, such as temperature, pH, and complex material geometries and surface morphology. We have carried out a surrogate simulation of the carbonation reaction process, in which a tobermorite nanoparticle (TNP) is placed in a mixture of H_2O and CO_2 molecules. The system temperature is relaxed at 300 K first, then subsequently heated to 1,200 K. The temperature is kept at 1,200 K using the *NVT* ensemble to accelerate the overall reaction. Figure 5a shows the initial shape of TNP. After elevating the temperature to 1,200 K, we observe the formation of carbonate and bicarbonate molecules around TNP (see Figure 5b). After 0.16 ns, active leaching of Ca and TNP dissolution are observed (see Figure 5c). The obtained MD trajectory was robust, and no spurious event such as overlapping atoms nor abrupt simulation failure was observed.

While the above fracture and nanoparticle-dissolution simulations demonstrate the robust generalizability of Allegro-FM to nonequilibrium MD simulations, practical applications involving nontrivial microstructures will require million-to-billion atom MD simulations.[33,60] We have confirmed the scalability of Allegro-FM on an exaflop/s parallel supercomputer. Namely, we have achieved 97.5% of the perfect speedup for 4.08 billion atoms on 4,096 graphics processing units (GPUs) on the Aurora supercomputer at Aronne Leadership Computing Facility (ALCF) (see Figure S2 in the Supporting Information).

Allegro-FM can perform versatile tasks beyond the original distribution of training data sets, as evidenced by the simulations of activation energy, tensile test, and TNP reactions. Though the force loss obtained in this study (130 meV/Å) is roughly three times higher than a guideline proposed by Chmiela et al.,[61] Allegro-FM exhibits a robust predictability and generalizability for reactions that are important in the geochemical cycle and cement chemistry, indicating the capability of Allegro-FM even without fine-tuning. Unlike a conventional ML model that is trained for a narrowly defined task, Allegro-FM is compatible with 89 elements in the periodic table. Therefore, incorporating other important metals such as Al, Fe, Mg, and Ti into the aforementioned calculations does not require time-consuming data generation or expensive model training from scratch. As an example, our preliminary results show that Allegro-FM can be effectively fine-tuned to a new data set aligned with the TEA framework without compromising the original accuracy. Since the size of the additional training set is usually much smaller, roughly 10% of original training data, it requires much less resources, e.g., 3 days on 8 NVIDIA A100 GPUs for initial training vs. 24 h on a single A100 for fine-tuning. Yet, we also note that Allegro-FM is not a universal force field that can be used as a black box. We have observed suboptimal performance for magnesium silicate systems with the current models,

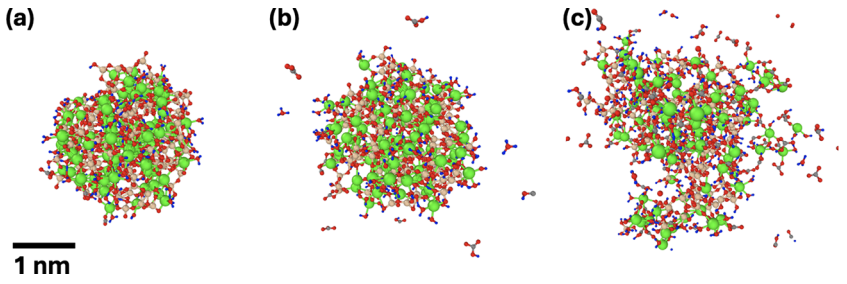

Figure 5. Snapshots of a tobermorite nanoparticle (TNP) placed in a mixture of H_2O and CO_2 molecules. Ca, Si, C, O, and H atoms are color-coded as green, khaki, gray, red, and blue, respectively. H_2O and CO_2 molecules are not shown for clarity. (a) Original TNP. (b) Shape of NP right after the system temperature is increased to 1,200 K. A noticeable formation of CO_3 and CO_3H molecules around the NP is observed. (c) After 0.16 ns, many Ca atoms dissolve from the NP into the H_2O and CO_2 mixture.

https://doi.org/10.1021/acs.jpclett.5c00605
J. Phys. Chem. Lett. 2025, 16, 6637−6644

Table 1. Hyperparameter Settings and the Total Number of Trainable Parameters for Each Allegro-FM Model

	Number of tensor feature	Latent dimensions	Two_body dimensions	Edge_eng dimensions	Number of parameters
Allegro-FM64	16	[64, 64, 64]	[16, 32, 64]	[64]	44.4K
Allegro-FM256	64	[256, 256, 256]	[64, 128, 256]	[128]	690K
Allegro-FM512	128	[512, 512, 512]	[128, 256, 512]	[128]	2.6M

in which the prediction accuracy may be enhanced by fine-tuning.

Equipped with the robust predictability, generalizability, computational efficiency, and algorithmic scalability, Allegro-FM has great potential for dynamical simulations spanning the micrometer spatial extent for microseconds time scale without sacrificing the atomistic details. This framework may be used to study the nanostructure of calcium silicate gel,[62] reaction-induced fracture,[63] self-healing cement,[64] and durable cement design,[36] thereby providing a novel atomistic simulation approach for geophysical science and civil engineering applications.

METHODS

The electronic states were calculated using the projector augmented method (PAW)[65,66] within the framework of the density functional theory (DFT) in which the generalized gradient approximation (GGA-PBE)[67] was used for the exchange−correlation energy. The planewave cutoff energies for the pseudo wave function and pseudo charge density were 30 and 200 Ry for tobermorite system and 30 and 250 Ry for the H_2O-CO_2 system, respectively. In the MD simulations, the equations of motion for atoms were solved via an explicit reversible integrator with a time step of Δt = 0.48 fs. The $g(r)$ in Figure 2 was obtained by averaging over 0.72 ps after the initial equilibration, which takes 0.24 ps. For the tensile simulation in Figure 4, the system was thermalized at 300 K in the canonical ensemble and subjected to tensile strain in the z-direction with a strain rate of 1×10^{10} s^{-1}. Further details of fracture simulations schedule are provided elsewhere.[68] For each applied strain, the system was simulated in the NVT ensemble for 0.48 ps. After the stress stabilized, the stress value for that strain was calculated by averaging over the last 0.29 ps.

The Allegro potential was implemented through NequIP, incorporating an E(3) symmetry equivariant neural network coded by e3nn[69] on the PyTorch framework. The model architecture, in the case of Allegro-FM256, consists of two layers of 64 tensor features with l = 2 in full O(3) symmetry. The network utilizes several multilayer perceptrons (MLPs) with specific configurations: a two-body latent MLP with dimensions [64, 128, 256] and a later latent MLP with dimensions [256, 256, 256], both employing SiLU non-linearities. Table 1 presents the specifications of each model used in this study. The embedding MLP was implemented as a linear projection, while the final edge energy MLP comprised a single hidden layer without nonlinearity. All MLPs were initialized according to a uniform distribution of unit variance. The training protocol employed a radial cutoff of 5.2 Å, with the loss function combining the per-atom energy, force, and stress root-mean-square errors under 8:1:1 weight ratio. Parameter optimization was performed using the Adam optimizer. All calculations were performed using Sophia at the Argonne Leadership Computing Facility.

In this study, the Total Energy Alignment (TEA) framework introduced by Shiota et al.[26] is used to train the Allegro network. TEA harmonizes heterogeneous quantum chemical data sets through a two-step process: Inner Core Energy Alignment (ICEA) and Atomization Energy Correction (AEC). ICEA addresses systematic energy offsets arising from different core electron treatments, while AEC scales atomization energies to account for varying computational fidelities. This methodology enables seamless integration of data sets computed under different conditions without extensive recalculations.

We utilized two complementary data sets to proceed through the TEA method: the inorganic structure MPtrj data set (calculated at PBE/PW level using VASP) and the OFF23 data set of organic molecules (computed at ωB97M-D3(BJ)/def2-TZVPPD level using Psi4). The publicly available integrated data set[70] was preprocessed by removing structures containing noble gas elements and those with forces exceeding 0.25 hartree to ensure stable training. This curated data set was then used to train the Allegro network.

During training, we monitored both the overall loss convergence and elementwise training performance. The model achieved a root-mean-square error of 117 meV for per atom energies, 130 meV/Å for forces, and 16 MPa for stress on the test data set.

We first created a bulk amorphous tobermorite using CLAYFF,[68] then cut out a tobermorite nanoparticle with a radius of 1.2 nm. The nanoparticles were placed in a mixture of H_2O and CO_2 molecules with a 50:50 ratio at a density of 1 g/cm^3. The cubic MD system of $(4.57\ \text{nm})^3$ contains 267 C, 90 Ca, 133 Si, 2577 O, and 3259 H atoms, respectively. The system is relaxed at 300 K using the *NVT* ensemble with 0.5 fs time step and then subsequently heated to 1,200 K in 22 ps. All simulations are performed using RXMD software.[71]

ASSOCIATED CONTENT

Supporting Information

The Supporting Information is available free of charge at https://pubs.acs.org/doi/10.1021/acs.jpclett.5c00605.

Tensile loading simulation along the *a*-axis of tobermorite 11Å crystal (Figure S1); effect of model hyperparameters and random number seed on the carbonic acid reaction pathways (Figure S2); training performance on reaction barrier and reaction energy evaluated by Transition1x data sets (Table S1); weak and scaling performance of Allegro-FM measured on Aurora supercomputer at Argonne Leadership Computing Facility (Figure S3) (PDF)

AUTHOR INFORMATION

Corresponding Authors

Ken-ichi Nomura − *Collaboratory for Advanced Computing and Simulation, University of Southern California, Los Angeles, California 90089-0242, United States;* orcid.org/0000-0002-1743-1419; Email: knomura@usc.edu

Shinnosuke Hattori − *Advanced Research Laboratory, Research Platform, Sony Group Corporation, Atsugi,*

https://doi.org/10.1021/acs.jpclett.5c00605
J. Phys. Chem. Lett. 2025, 16, 6637−6644

Kanagawa 243-0014, Japan; orcid.org/0000-0003-0786-1308; Email: shinnosuke.hattori@sony.com

Authors

Satoshi Ohmura − *Premier Institute for Advanced Studies, Ehime University, Matsuyama 790-8577, Japan*

Ikumi Kanemasu − *Department of Physics, Ehime University, Matsuyama 790-8577, Japan*

Kohei Shimamura − *Department of Physics, Kumamoto University, Kumamoto 860-8555, Japan;* orcid.org/0000-0003-3235-2599

Nabankur Dasgupta − *Collaboratory for Advanced Computing and Simulation, University of Southern California, Los Angeles, California 90089-0242, United States;* orcid.org/0000-0002-5262-6086

Aiichiro Nakano − *Collaboratory for Advanced Computing and Simulation, University of Southern California, Los Angeles, California 90089-0242, United States;* orcid.org/0000-0003-3228-3896

Rajiv K. Kalia − *Collaboratory for Advanced Computing and Simulation, University of Southern California, Los Angeles, California 90089-0242, United States*

Priya Vashishta − *Collaboratory for Advanced Computing and Simulation, University of Southern California, Los Angeles, California 90089-0242, United States;* orcid.org/0000-0003-4683-429X

Complete contact information is available at: https://pubs.acs.org/10.1021/acs.jpclett.5c00605

Notes

The authors declare no competing financial interest.

■ ACKNOWLEDGMENTS

This research was supported by the U.S. Department of Energy, Office of Basic Energy Sciences, Chemical Sciences, Geosciences, and Bioscience Division, Geosciences Program under Award DE-SC0025222. S.O. and K.S. acknowledges support from the JSPS KAKENHI (Nos. 24K07630 and 22K03454). Scalability tests on the Aurora supercomputers at the Argonne Leadership Computing Facility were performed under the Aurora Early Science Program (ESP) U.S. DOE Innovative and Novel Computational Impact on Theory and Experiment (INCITE) Program. This research used resources from the Argonne Leadership Computing Facility, a U.S. DOE Office of Science user facility at Argonne National Laboratory, which is supported by the Office of Science of the U.S. DOE under Contract No. DE-AC02-06CH11357.

■ REFERENCES

(1) Bommasani, R.; Hudson, D. A.; Adeli, E.; Altman, R.; Arora, S.; von Arx, S.; Bernstein, M. S.; Bohg, J.; Bosselut, A.; Brunskill, E.; et al. On the Opportunities and Risks of Foundation Models. *arXiv* **2021**, No. 2108.07258.

(2) Brown, T. B.; Mann, B.; Ryder, N.; Subbiah, M.; Kaplan, J.; Dhariwal, P.; Neelakantan, A.; Shyam, P.; Sastry, G.; Askell, A.; Agarwal, S.; et al. Language Models Are Few-Shot Learners. *arXiv* **2020**, *2005*, No. 14165.

(3) OpenAI; Achiam, J.; Adler, S.; Agarwal, S.; Ahmad, L.; Akkaya, I.; Aleman, F. L.; Almeida, D.; Altenschmidt, J.; et al. GPT-4 Technical Report. *arXiv* **2023**, No. 2303.08774.

(4) Team, Gemini; Anil, R.; Borgeaud, S.; Alayrac, J.-B.; Yu, J.; Soricut, R.; Schalkwyk, J.; Dai, A. M.; Hauth, A.; Millican, K.; et al. Gemini: A Family of Highly Capable Multimodal Models. *arXiv* **2023**, No. 2312.11805.

(5) Touvron, H.; Lavril, T.; Izacard, G.; Martinet, X.; Lachaux, M.-A.; Lacroix, T.; Rozière, B.; Goyal, N.; Hambro, E.; Azhar, F.; Rodriguez, A.; Joulin, A.; Grave, E.; Lample, G. LLaMA: Open and Efficient Foundation Language Models. *arXiv* **2023**, No. 2302.13971.

(6) Takeda, S.; Kishimoto, A.; Hamada, L.; Nakano, D.; Smith, J. R. Foundation Model for Material Science. *Proc. Conf. AAAI Artif. Intell.* **2023**, *37* (13), 15376−15383.

(7) Takeda, S.; Priyadarsini, I.; Kishimoto, A.; Shinohara, H.; Hamada, L.; Masataka, H.; Fuchiwaki, J.; Nakano, D. Multi-Modal Foundation Model for Material Design. In *AI for Accelerated Materials Design - NeurIPS 2023 Workshop*; Conference and Workshop on Neural Information Processing Systems, 2023.

(8) Vaswani, A.; Shazeer, N. M.; Parmar, N.; Uszkoreit, J.; Jones, L.; Gomez, A. N.; Kaiser, L.; Polosukhin, I. Attention Is All You Need. *Neural Inf Process Syst* **2017**, 5998−6008.

(9) Deng, B.; Zhong, P.; Jun, K.; Riebesell, J.; Han, K.; Bartel, C. J.; Ceder, G. CHGNet as a Pretrained Universal Neural Network Potential for Charge-Informed Atomistic Modelling. *Nat. Mach. Intell.* **2023**, *5* (9), 1031−1041.

(10) Jain, A.; Ong, S. P.; Hautier, G.; Chen, W.; Richards, W. D.; Dacek, S.; Cholia, S.; Gunter, D.; Skinner, D.; Ceder, G.; Persson, K. A. Commentary: The Materials Project: A Materials Genome Approach to Accelerating Materials Innovation. *APL Mater.* **2013**, *1* (1), No. 011002.

(11) Eastman, P.; Behara, P. K.; Dotson, D. L.; Galvelis, R.; Herr, J. E.; Horton, J. T.; Mao, Y.; Chodera, J. D.; Pritchard, B. P.; Wang, Y.; De Fabritiis, G.; Markland, T. E. SPICE, A Dataset of Drug-like Molecules and Peptides for Training Machine Learning Potentials. *Sci. Data* **2023**, *10* (1), 11.

(12) Ghahremanpour, M. M.; van Maaren, P. J.; van der Spoel, D. The Alexandria Library, a Quantum-Chemical Database of Molecular Properties for Force Field Development. *Sci. Data* **2018**, *5* (1), 180062.

(13) Kirklin, S.; Saal, J. E.; Meredig, B.; Thompson, A.; Doak, J. W.; Aykol, M.; Rühl, S.; Wolverton, C. The Open Quantum Materials Database (OQMD): Assessing the Accuracy of DFT Formation Energies. *Npj Comput. Mater.* **2015**, *1* (1), 1−15.

(14) Curtarolo, S.; Setyawan, W.; Wang, S.; Xue, J.; Yang, K.; Taylor, R. H.; Nelson, L. J.; Hart, G. L. W.; Sanvito, S.; Buongiorno-Nardelli, M.; Mingo, N.; Levy, O. AFLOWLIB.ORG: A Distributed Materials Properties Repository from High-Throughput Ab Initio Calculations. *Comput. Mater. Sci.* **2012**, *58*, 227−235.

(15) Drautz, R. Atomic Cluster Expansion for Accurate and Transferable Interatomic Potentials. *Phys. Rev. B* **2019**, *99* (1), No. 014104.

(16) Batatia, I.; Kovács, D. P.; Simm, G. N. C.; Ortner, C.; Csányi, G. MACE: Higher Order Equivariant Message Passing Neural Networks for Fast and Accurate Force Fields. *arXiv* **2022**, No. 2206.07697.

(17) Batzner, S.; Musaelian, A.; Sun, L.; Geiger, M.; Mailoa, J. P.; Kornbluth, M.; Molinari, N.; Smidt, T. E.; Kozinsky, B. E(3)-Equivariant Graph Neural Networks for Data-Efficient and Accurate Interatomic Potentials. *Nat. Commun.* **2022**, *13* (1), 2453.

(18) Liao, Y.-L.; Smidt, T. Equiformer: Equivariant Graph Attention Transformer for 3d Atomistic Graphs. *arXiv* **2022**, No. 2206.11990.

(19) Liao, Y.-L.; Wood, B.; Das, A.; Smidt, T. EquiformerV2: Improved Equivariant Transformer for Scaling to Higher-Degree Representations. *arXiv* **2023**, No. 2306.12059.

(20) Neumann, M.; Gin, J.; Rhodes, B.; Bennett, S.; Li, Z.; Choubisa, H.; Hussey, A.; Godwin, J. Orb: A Fast, Scalable Neural Network Potential. *arXiv* **2024**, No. 2410.22570.

(21) Zeni, C.; Pinsler, R.; Zügner, D.; Fowler, A.; Horton, M.; Fu, X.; Wang, Z.; Shysheya, A.; Crabbé, J.; Ueda, S.; Sordillo, R.; Sun, L.; Smith, J.; Nguyen, B.; Schulz, H.; Lewis, S.; Huang, C.-W.; Lu, Z.; Zhou, Y.; Yang, H.; Hao, H.; Li, J.; Yang, C.; Li, W.; Tomioka, R.; Xie, T. A Generative Model for Inorganic Materials Design. *Nature* **2025**, *639*, 624.

(22) Riebesell, J.; Goodall, R. E. A.; Benner, P.; Chiang, Y.; Deng, B.; Ceder, G.; Asta, M.; Lee, A. A.; Jain, A.; Persson, K. A. Matbench

Discovery – A Framework to Evaluate Machine Learning Crystal Stability Predictions. *arXiv* **2023**, No. 2308.14920.
(23) Miret, S.; Lee, K. L. K.; Gonzales, C.; Mannan, S.; Krishnan, N. M. A. Energy & Force Regression on DFT Trajectories Is Not Enough for Universal Machine Learning Interatomic Potentials. *arXiv* **2025**, No. 2502.03660.
(24) Musaelian, A.; Batzner, S.; Johansson, A.; Sun, L.; Owen, C. J.; Kornbluth, M.; Kozinsky, B. Learning Local Equivariant Representations for Large-Scale Atomistic Dynamics. *Nat. Commun.* **2023**, *14* (1), 579.
(25) Kovács, D. P.; Moore, J. H.; Browning, N. J.; Batatia, I.; Horton, J. T.; Kapil, V.; Magdău, I.-B.; Cole, D. J.; Csányi, G. MACE-OFF23: Transferable Machine Learning Force Fields for Organic Molecules. *arXiv* **2023**, No. 2312.15211.
(26) Shiota, T.; Ishihara, K.; Do, T. M.; Mori, T.; Mizukami, W. Taming Multi-Domain, -Fidelity Data: Towards Foundation Models for Atomistic Scale Simulations. *arXiv* **2024**, No. 2412.13088.
(27) Ibayashi, H.; Razakh, T. M.; Yang, L.; Linker, T.; Olguin, M.; Hattori, S.; Luo, Y.; Kalia, R. K.; Nakano, A.; Nomura, K.; Vashishta, P. Allegro-Legato: Scalable, Fast, and Robust Neural-Network Quantum Molecular Dynamics via Sharpness-Aware Minimization. In *High Performance Computing*; Springer Nature Switzerland, 2023; pp 223−239.
(28) Nakano, A.; Kalia, R. K.; Sharma, A.; Vashishta, P.; Ogata, S.; Shimojo, F. Virtualization-Aware Application Framework for Hierarchical Multiscale Simulations on a Grid. In *Computational Methods in Large Scale Simulation*; Lecture Notes Series. Institute for Mathematical Sciences. National University of Singapore. 2005; pp 229−243.
(29) Zwanzig, R. W. High-Temperature Equation of State by a Perturbation Method. I. Nonpolar Gases. *J. Chem. Phys.* **1954**, *22* (8), 1420−1426.
(30) Warshel, A.; Levitt, M. Theoretical Studies of Enzymic Reactions - Dielectric, Electrostatic and Steric Stabilization of Carbonium-Ion in Reaction of Lysozyme. *J. Mol. Biol.* **1976**, *103* (2), 227−249.
(31) Dapprich, S.; Komaromi, I.; Byun, K.S.; Morokuma, K.; Frisch, M. J A New ONIOM Implementation in Gaussian98. Part I. The Calculation of Energies, Gradients, Vibrational Frequencies and Electric Field Derivatives. *Journal of Molecular Structure: THEOCHEM* **1999**, *461−462*, 1−21.
(32) Kozinsky, B.; Musaelian, A.; Johansson, A.; Batzner, S. Scaling the Leading Accuracy of Deep Equivariant Models to Biomolecular Simulations of Realistic Size. In *Proceedings of the International Conference for High Performance Computing, Networking, Storage and Analysis*; SC '23; Association for Computing Machinery: New York, NY, USA, 2023; pp 1−12.
(33) Shekhar, A.; Nomura, K.; Kalia, R. K.; Nakano, A.; Vashishta, P. Nanobubble Collapse on a Silica Surface in Water: Billion-Atom Reactive Molecular Dynamics Simulations. *Phys. Rev. Lett.* **2013**, *111* (18), 184503.
(34) Linker, T.; Nomura, K.; Aditya, A.; Fukshima, S.; Kalia, R. K.; Krishnamoorthy, A.; Nakano, A.; Rajak, P.; Shimmura, K.; Shimojo, F.; Vashishta, P. Exploring Far-from-Equilibrium Ultrafast Polarization Control in Ferroelectric Oxides with Excited-State Neural Network Quantum Molecular Dynamics. *Science Advances* **2022**, *8* (12), No. eabk2625.
(35) Chen, Y.-C.; Lu, Z.; Nomura, K.; Wang, W.; Kalia, R. K.; Nakano, A.; Vashishta, P. Interaction of Voids and Nanoductility in Silica Glass. *Phys. Rev. Lett.* **2007**, *99* (15), No. 155506.
(36) Seymour, L. M.; Maragh, J.; Sabatini, P.; Di Tommaso, M.; Weaver, J. C.; Masic, A. Hot Mixing: Mechanistic Insights into the Durability of Ancient Roman Concrete. *Sci. Adv.* **2023**, *9* (1), No. eadd1602.
(37) Jackson, M. D.; Chae, S. R.; Mulcahy, S. R.; Meral, C.; Taylor, R.; Li, P.; Emwas, A.-H.; Moon, J.; Yoon, S.; Vola, G.; Wenk, H.-R.; Monteiro, P. J. M. Unlocking the Secrets of Al-Tobermorite in Roman Seawater Concrete. *Am. Mineral.* **2013**, *98* (10), 1669−1687.
(38) Seifritz, W. CO2 Disposal by Means of Silicates. *Nature* **1990**, *345*, 486−486.
(39) Berner, R. A.; Lasaga, A. C.; Garrels, R. M. The Carbonate-Silicate Geochemical Cycle and Its Effect on Atmospheric Carbon Dioxide over the Past 100 Million Years. *Am. J. Sci.* **1983**, *283* (7), 641−683.
(40) Chen, Y.; Kanan, M. W. Thermal Ca2+/Mg2+ Exchange Reactions to Synthesize CO2 Removal Materials. *Nature* **2025**, *638*, 972.
(41) Fu, X.; Guerini, A.; Zampini, D.; Rotta Loria, A. F. Storing CO2 While Strengthening Concrete by Carbonating Its Cement in Suspension. *Commun. Mater.* **2024**, *5* (1), 1−14.
(42) Car, R.; Parrinello, M. Unified Approach for Molecular Dynamics and Density-Functional Theory. *Phys. Rev. Lett.* **1985**, *55* (22), 2471−2474.
(43) Payne, M. C.; Teter, M. P.; Allan, D. C.; Arias, T. A.; Joannopoulos, J. D. Iterative Minimization Techniques for Ab Initio Total-Energy Calculations: Molecular Dynamics and Conjugate Gradients. *Rev. Mod. Phys.* **1992**, *64* (4), 1045−1097.
(44) Hohenberg, P.; Kohn, W. Inhomogeneous Electron Gas. *Phys. Rev.* **1964**, *136* (3B), B864−B871.
(45) Kohn, W.; Sham, L. J. Self-Consistent Equations Including Exchange and Correlation Effects. *Phys. Rev.* **1965**, *140* (4A), A1133−A1138.
(46) Cygan, R. T.; Liang, J.-J.; Kalinichev, A. G. Molecular Models of Hydroxide, Oxyhydroxide, and Clay Phases and the Development of a General Force Field. *J. Phys. Chem. B* **2004**, *108* (4), 1255−1266.
(47) Cygan, R. T.; Greathouse, J. A.; Kalinichev, A. G. Advances in Clayff Molecular Simulation of Layered and Nanoporous Materials and Their Aqueous Interfaces. *J. Phys. Chem. C Nanomater. Interfaces* **2021**, *125* (32), 17573−17589.
(48) Richardson, I. G. The Calcium Silicate Hydrates. *Cem. Concr. Res.* **2008**, *38* (2), 137−158.
(49) Duque-Redondo, E.; Bonnaud, P. A.; Manzano, H. A Comprehensive Review of C-S-H Empirical and Computational Models, Their Applications, and Practical Aspects. *Cem. Concr. Res.* **2022**, *156*, 106784.
(50) Shahsavari, R.; Pellenq, R. J.-M.; Ulm, F.-J. Empirical Force Fields for Complex Hydrated Calcio-Silicate Layered Materials. *Phys. Chem. Chem. Phys.* **2011**, *13* (3), 1002−1011.
(51) Shahsavari, R.; Buehler, M. J.; Pellenq, R. J.-M.; Ulm, F.-J. First-Principles Study of Elastic Constants and Interlayer Interactions of Complex Hydrated Oxides: Case Study of Tobermorite and Jennite. *J. Am. Ceram. Soc.* **2009**, *92* (10), 2323−2330.
(52) Henkelman, G.; Uberuaga, B. P.; Jónsson, H. A Climbing Image Nudged Elastic Band Method for Finding Saddle Points and Minimum Energy Paths. *J. Chem. Phys.* **2000**, *113* (22), 9901−9904.
(53) Schreiner, M.; Bhowmik, A.; Vegge, T.; Busk, J.; Winther, O. Transition1x - a Dataset for Building Generalizable Reactive Machine Learning Potentials. *Sci. Data* **2022**, *9* (1), 779.
(54) Fu, X.; Wu, Z.; Wang, W.; Xie, T.; Keten, S.; Gomez-Bombarelli, R.; Jaakkola, T. Forces Are Not Enough: Benchmark and Critical Evaluation for Machine Learning Force Fields with Molecular Simulations. *arXiv* **2022**, No. 2210.07237.
(55) Lu, Z.; Nomura, K.; Sharma, A.; Wang, W.; Zhang, C.; Nakano, A.; Kalia, R.; Vashishta, P.; Bouchaud, E.; Rountree, C. Dynamics of Wing Cracks and Nanoscale Damage in Glass. *Phys. Rev. Lett.* **2005**, *95* (13), 135501.
(56) Chen, Y.-C.; Nomura, K.; Kalia, R. K.; Nakano, A.; Vashishta, P. Void Deformation and Breakup in Shearing Silica Glass. *Phys. Rev. Lett.* **2009**, *103* (3), No. 035501.
(57) Nomura, K.; Chen, Y.-C.; Kalia, R. K.; Nakano, A.; Vashishta, P. Defect Migration and Recombination in Nanoindentation of Silica Glass. *Appl. Phys. Lett.* **2011**, *99* (11).111906
(58) Nomura, K.; Mishra, A.; Sang, T.; Kalia, R. K.; Nakano, A.; Vashishta, P. Molecular Autonomous Pathfinder Using Deep Reinforcement Learning. *J. Phys. Chem. Lett.* **2024**, *15* (19), 5288−5294.

https://doi.org/10.1021/acs.jpclett.5c00605
J. Phys. Chem. Lett. 2025, 16, 6637−6644

(59) Mutisya, S. M.; Miranda, C. R. The Surface Stability and Morphology of Tobermorite 11 Å from First Principles. *Appl. Surf. Sci.* **2018**, *444*, 287−292.
(60) Nomura, K.; Kalia, R. K.; Li, Y.; Nakano, A.; Rajak, P.; Sheng, C.; Shimamura, K.; Shimojo, F.; Vashishta, P. Nanocarbon Synthesis by High-Temperature Oxidation of Nanoparticles. *Sci. Rep.* **2016**, *6*, 24109.
(61) Chmiela, S.; Sauceda, H. E.; Muller, K. R.; Tkatchenko, A. Towards Exact Molecular Dynamics Simulations with Machine-Learned Force Fields. *Nat. Commun.* **2018**, *9*. DOI: 10.1038/s41467-018-06169-2
(62) Yan, Y.; Geng, G. Does Nano Basic Building-Block of C-S-H Exist?−A Review of Direct Morphological Observations. *Mater. Des.* **2024**, *238*, 112699.
(63) Zhu, W.; Fusseis, F.; Lisabeth, H.; Xing, T.; Xiao, X.; De Andrade, V.; Karato, S.-I. Experimental Evidence of Reaction-Induced Fracturing during Olivine Carbonation. *Geophys. Res. Lett.* **2016**, *43* (18), 9535−9543.
(64) Alex, A.; Freeman, B.; Jefferson, A.; Masoero, E. Carbonation and Self-Healing in Concrete: Kinetic Monte Carlo Simulations of Mineralization. *Cem. Concr. Compos.* **2023**, *144*, 105281.
(65) Blöchl, P. E. Projector Augmented-Wave Method. *Phys. Rev. B* **1994**, *50* (24), 17953−17979.
(66) Kresse, G.; Joubert, D. From Ultrasoft Pseudopotentials to the Projector Augmented-Wave Method. *Phys. Rev. B* **1999**, *59* (3), 1758−1775.
(67) Perdew, J. P.; Burke, K.; Ernzerhof, M. Generalized Gradient Approximation Made Simple. *Phys. Rev. Lett.* **1996**, *77* (18), 3865−3868.
(68) Kanemasu, I.; Ohmura, S.; Takeda, N.; Shimojo, F. Mechanical Properties of Layered Structure of 1.1-Nm Tobermorite Using Ab Initio Molecular Dynamics Simulation. *Cement science and concrete technology* **2025**, *78*, 18−25.
(69) Geiger, M.; Smidt, T. e3nn: Euclidean Neural Networks. *arXiv* **2022**, No. 2207.09453.
(70) MACE Osaka24 Models. https://github.com/qiqb-osaka/mace-osaka24 (accessed 2025-05-06).
(71) Nomura, K.; Kalia, R. K.; Nakano, A.; Rajak, P.; Vashishta, P. RXMD: A Scalable Reactive Molecular Dynamics Simulator for Optimized Time-to-Solution. *SoftwareX* **2020**, *11*, 100389.

https://doi.org/10.1021/acs.jpclett.5c00605
J. Phys. Chem. Lett. 2025, 16, 6637−6644